Beam Models for Nonlinear and Time-Dependent Analysis of Curved Prestressed Box Girder Bridges

ANTONIO R. MARÍ, SERGIO CARRASCÓN, AND ANGEL LOPEZ

Two analytical models developed to study the structural response of curved prestressed concrete box girder bridges are presented. The first one consists of a filament beam model, with arbitrary longitudinal and sectional geometry. Concrete and steel are assumed to be subjected to a uniaxial stress state. Material nonlinearities such as cracking of concrete, yielding of steel, and so forth are taken into account. Flexural and torsional behaviors are considered uncoupled. Time-dependent effects due to load history, creep, shrinkage, and aging of concrete and relaxation of prestressing steel are also included. In the second approach, a box-beam straight element of nondeformable cross section composed of concrete panels with steel layers is used to model the bridge. Concrete is assumed to be subjected to a biaxial stress state. Material nonlinearities are also considered. Longitudinal and transverse prestressing can be included. Coupling between flexural, torsional, and shear response of the cross section is considered. A curved prestressed box girder bridge constructed in Spain is analyzed by the two models presented under different loading conditions. Short-term analyses with increasing overload to failure demonstrate the applicability of the uncoupled model when either bending or torsion is dominant, whereas for other cases coupling is necessary to accurately predict the structural response. A time-dependent analysis under permanent loads is made, followed by a long-term overload analysis showing the effects of time in the structural response. The influence of transverse prestressing on the structural behavior is also studied.

In recent years reinforced and prestressed concrete curved box girder bridges have been widely used for overcrossings and viaducts. Characteristic features that have made box girders an attractive alternative for bridge designers include their structural efficiency (high flexural and torsional stiffness combined with light weight) and their pleasing aesthetic qualities (the clean lines of the closed section and the ability to use single, slender piers as supports).

Present and past designs of box girder bridges have usually been based on linear elastic analysis using simplified models of uncracked, homogeneous systems. These models are able to predict adequately the behavior of prestressed concrete bridges at service load levels. However, if such a structure is loaded beyond the working stress range, excessive cracking of the concrete and eventual yielding of the reinforcement no longer justify the use of linear elastic models.

In addition, bending and torsional moments in curved bridges are coupled, which means that the bending moment and torque cannot be obtained separately. When a section subjected to combined actions cracks, its stiffness decreases significantly. Generally the loss of torsional stiffness is proportionally greater than the loss of flexural stiffness, so the structural response under increasing load will be nonlinear after cracking.

In curved prestressed concrete bridges over simple intermediate supports, very high torsional moments are originated, particularly under certain loading cases (if only the exterior lanes are loaded). The longitudinal prestressing designed to prevent flexural cracking at service load levels may not be sufficient to avoid cracking caused by torsion, so the girder flanges are usually prestressed transversely. Such prestressing will influence the torsional response and therefore the overall structural behavior.

Time-dependent effects such as creep and shrinkage of concrete and relaxation of prestressing steel may change the prestressing force of the tendons as well as the stresses and strains of concrete and steel. Consequently the structural response under increasing load up to failure will depend, to a certain extent, on the load history.

It is evident that a complete understanding of such complex structural behavior requires an important effort from the experimental and theoretical viewpoints. In this paper, two mathematical models developed by the authors (*1*, *2*) for the nonlinear analysis of reinforced and prestressed concrete curved box girder bridges are briefly described. The paper will focus particularly on the structural response of a curved prestressed box girder bridge, drawing conclusions regarding the behavior of such structures and the applicability of the proposed analytical models.

DESCRIPTION OF ANALYTICAL MODELS

General Remarks: Common Assumptions

The behavior of single box girder bridges can be reasonably simulated by means of beam theory when the ratio of span to cell width is greater than approximately 5. In such a range of span–cell-width ratio, the influence of transverse distortion and warping of the cross section on the longitudinal stresses may be, for the usual prestressed concrete box girders, very small (*3*), which means that assumptions can be made about the nondeformability of sections in their plane, as well as about the deformation of Navier's plane sections.

Universitat Politècnica de Catalunya, Barcelona, Spain.

The analytical models developed can be described by attending essentially to four aspects: structural idealization, material models used, sectional analysis, and structural analysis. In the following, a brief description of the characteristics of each model is given.

Model 1: Filament Beam with Uncoupled Torsional-Flexural Behavior

Structural Idealization

The structures that can be analyzed with this model are general three-dimensional reinforced and prestressed concrete frames composed of prismatic or nonprismatic members, with arbitrary cross section, and straight or curved in space. The members are interconnected by structural nodes. Such nodes are strictly necessary only at the actual structural joints, not inside the element. However, for integration purposes, a number of sections along the member are considered, in which a local coordinate system is defined (Figure 1).

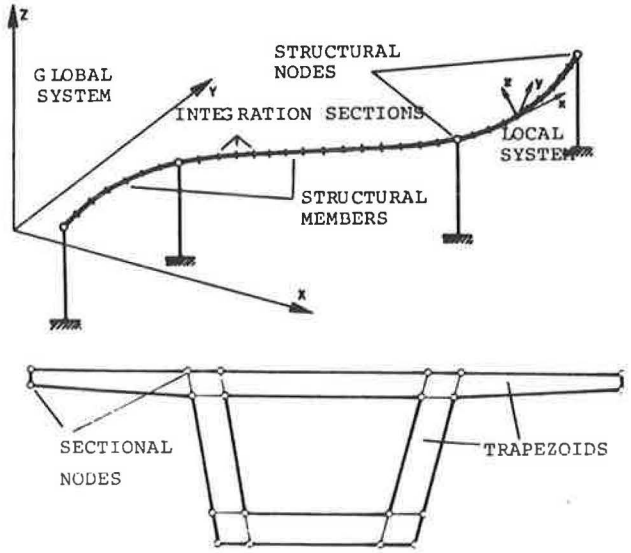

FIGURE 1 Structural idealization (Model 1).

Six degrees of freedom are considered at the end of each member: three translations and three rotations. Such longitudinal idealization allows the modeling of large structures with a small number of long elements, reducing the global matrix stiffness size at the expense of greater computer time because of the integration process along the bars.

Loads or moments can be applied either over the nodes or along the member length with any position and orientation in space. Imposed displacements and constraints at supported nodes can also be applied in any direction.

The cross section is discretized by means of trapezoids (Figure 1), each one defined by a four-sectional vertex. The trapezoids are made into squares by means of a parametric transformation. Then, a 5 × 5-point mesh over each square together with a two-dimensional Simpson rule are used for integration over the cross section. Mechanical properties as well as sectional forces can be obtained very accurately with this system.

Reinforcing steel bars are considered embedded elements parallel to the longitudinal member reference line. The area and position of each bar in local coordinates of the section are given as input data.

Pretensioned and posttensioned longitudinal tendons can be considered in this model. Each tendon can be extended to any length of the structure. A prestressing tendon may be composed of several segments, each of them of different profile (straight or parabolic, with or without end slope constraints). Jacking can be done from either of the two ends; friction losses and anchorage slip are taken into account.

Material Constitutive Equations

Concrete and steel are assumed to be subjected to a uniaxial longitudinal stress state. Total concrete strain at a given time and point in the structure is taken as the direct sum of mechanical strain (stress-produced strain) and nonmechanical strain, consisting of creep strain, shrinkage strain, and thermal strain.

The nonlinear constitutive relationship for concrete is shown in Figure 2a. This model is based on the one suggested by Sargin (*4*), including load reversal branches parallel to the initial slope. Eleven possible material states are considered.

For the reinforcing steel, a bilinear stress-strain relationship is assumed with load reversals, making four different material states, as shown in Figure 2b. A multilinear stress-strain curve is used for prestressing steel (Figure 2d). In addition, the usual empirical formulas are used for stress relaxation and friction properties of the prestressing steel.

Creep strain ε_c of concrete is evaluated by an age-dependent integral formulation based on the principle of superposition. Thus

$$\varepsilon_c(t) = \int_0^t c(t, t-\tau) \frac{\partial \sigma(\tau)}{\partial \tau} d\tau \qquad (1)$$

where $c(t, t - \tau)$ is the specific creep function, dependent on the age of loading. It can be seen from Equation 1 that for the determination of creep strain at any instant t, it is necessary to know all the stress history at each point. This problem can be avoided by using a Dirichlet series for the specific creep function, such as

$$c(t, t-\tau) = \sum_{i=1}^{n} a_i(\tau) \{1 - \exp[-\lambda_i (t-\tau)]\} \qquad (2)$$

where $a_i(\tau)$ and λ_i are parameters to be determined from experimental or empirical creep curves. Using such a creep function incorporates the historic effects by successively updating only one stress increment, instead of the entire stress history (*5*).

Sectional Analysis

The sectional deformation is characterized in this model by six components: axial strain of the reference sectional center, two flexural curvatures, an average twist, and two shear deformations.

In additional to Navier's plane-section hypothesis, uncoupling between normal and tangential responses and a perfect bond between steel and concrete are assumed.

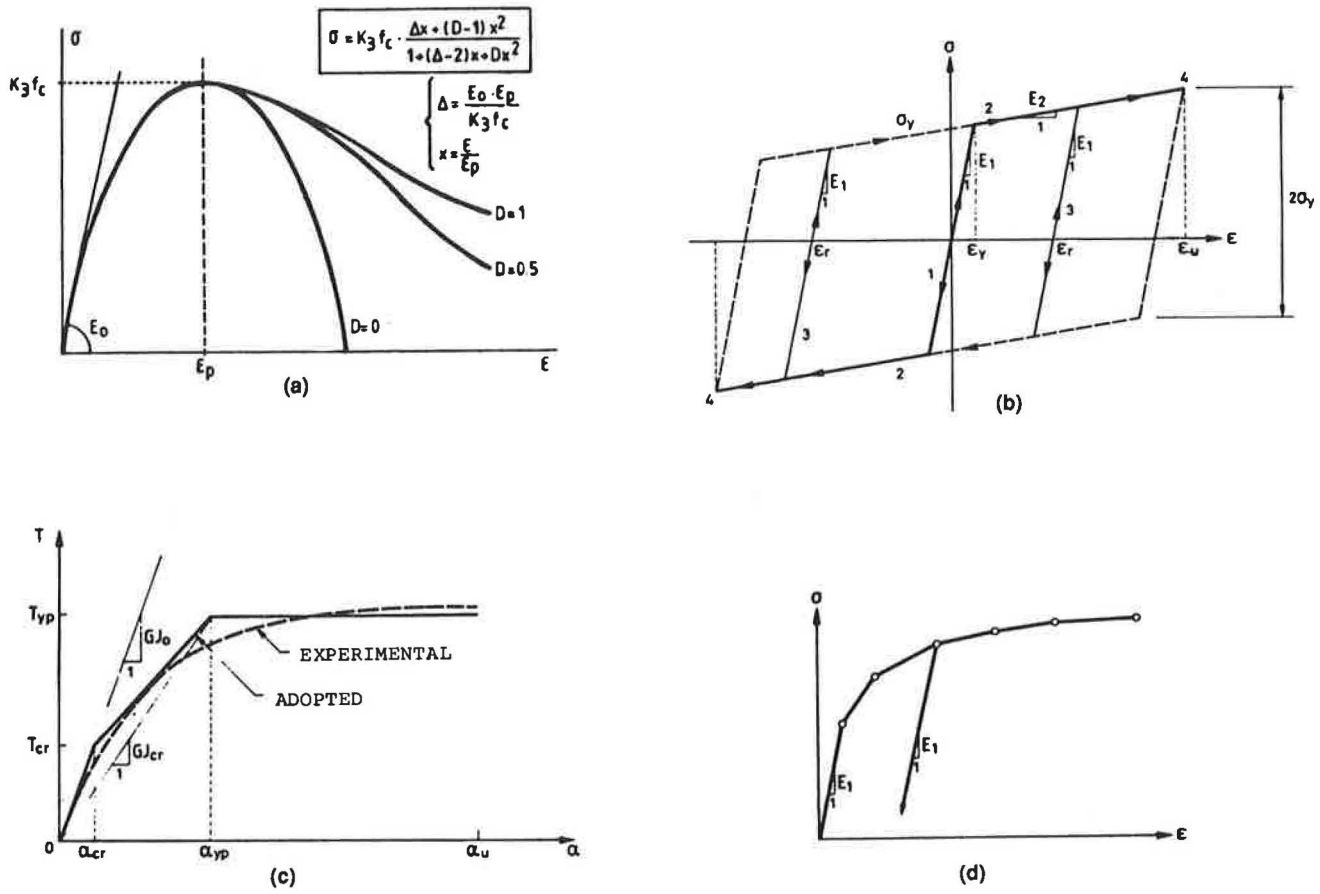

FIGURE 2 Material properties and torsional behavior (Model 1).

The sectional behavior can be expressed by a general constitutive equation derived by combining equilibrium equations between stresses and forces, compatibility of strains over the section, and material constitutive relations at each point. Such an equation, incrementally expressed, takes the following form:

$$\Delta\vec{\sigma}_s = \mathbf{k}_s \cdot \Delta\vec{\varepsilon}_s + \Delta\vec{\sigma}_s^0 \tag{3}$$

where $\Delta\vec{\sigma}_s$ is the vector of sectional forces, composed of axial force, two bending moments, torque, and two shear forces; $\Delta\vec{\varepsilon}_s$ is a vector of sectional deformations; $\Delta\vec{\sigma}_s^0$ is vector of initial stresses; and $\mathbf{k}_s$ is the tangent sectional stiffness matrix, which takes into account the material state at each point (cracked, yielded, crushed, etc.), including the contributions of reinforcing and prestressing steel. Therefore, material nonlinearities are included in the sectional stiffness matrix.

The uncoupling hypothesis leads to a sectional stiffness matrix such as the following:

$$\begin{pmatrix} \Delta N \\ \Delta M_y \\ \Delta M_z \\ \Delta T \\ \Delta V_y \\ \Delta V_z \end{pmatrix} = \begin{pmatrix} k_{11} & k_{12} & k_{13} & & & \\ & k_{22} & k_{23} & & \mathbf{0} & \\ & & k_{33} & & & \\ & & & k_{44} & k_{45} & k_{46} \\ & & & & k_{55} & k_{56} \\ & & & & & k_{66} \end{pmatrix} \begin{pmatrix} \Delta\varepsilon_0 \\ \Delta\phi_y \\ \Delta\phi_z \\ \Delta\alpha \\ \Delta\gamma_y \\ \Delta\gamma_z \end{pmatrix} + \begin{pmatrix} \Delta N^0 \\ \Delta M_y^0 \\ \Delta M_z^0 \\ \Delta T^0 \\ \Delta V_y^0 \\ \Delta V_z^0 \end{pmatrix} \tag{4}$$

in which the flexural forces are related only to longitudinal deformations.

The term k_{44} represents the torsional stiffness, which depends on the load level. In this model a trilinear torque-twist relationship is assumed in which k_{44} is the slope of such a diagram. The representative parameters of the torsional model are the initial stiffness GJ_0, the torque at first cracking T_{cr}, the cracked torsional stiffness k_{11}, the torque at full yielding T_{yp}, and the ultimate twist (*6*). Inelastic unloading parallel to the initial stiffness GJ_0 is assumed, as shown in Figure 2c.

Structural Analysis Procedure

The method of nonlinear structural analysis is developed on the basis of the classic matrix structural analysis of curved bars in space, extended to take into account material nonlinearities and time-dependent effects on reinforced and prestressed concrete three-dimensional frames.

The member stiffness matrix is derived by setting the three basic equations at the element level, expressed in global coordinates:

1. Incremental equilibrium equations:

$$\Delta\vec{\sigma}_{sxy}(s) = N(s) \cdot \Delta\vec{P}_B + \Delta\vec{\sigma}^*_{sxy}(s) \tag{5}$$

where

$\Delta\vec{\sigma}_{sxy}(s)$ = vector of internal forces at any section of the member;
$N(s)$ = equilibrium matrix, depending on the beam geometry;
$\Delta\vec{P}_B$ = vector of applied loads at one of the member ends; and
$\Delta\vec{\sigma}^*_{sxy}(s)$ = vector of forces acting at any section, caused by applied loads over the member, in a statically determinate configuration.

Such an equation comes from integration of the differential equilibrium equation of the beam, with the appropriate boundary conditions.

2. Incremental kinematic equations:

$$\Delta\vec{d} = \int_A^B N^T(s) \cdot \Delta\vec{\varepsilon}_{sxy}(s)\, ds \tag{6}$$

where $\Delta\vec{d}$ is the vector of relative displacements between both member ends, and the other terms are as defined previously.

3. Constitutive sectional Equation 3, transformed to global coordinates: If the above equations are combined and completed for the rest of the member degrees of freedom, the general member force-displacement relationship is obtained:

$$\Delta\vec{F} = K \cdot \Delta\vec{\delta} + \Delta\vec{F}^* + \Delta\vec{F}^0 \tag{7}$$

where

$\Delta\vec{F}$ = vector of applied loads at both member ends,
K = member tangent stiffness matrix,
$\Delta\vec{\delta}$ = vector of member end displacements,
$\Delta\vec{F}^*$ = vector of fixed end forces due to applied loads over the member length, and
$\Delta\vec{F}^0$ = vector of fixed end forces due to initial stresses.

By assembling the elementary equations for the complete structure, a similar global expression is obtained.

For the nonlinear time-dependent analysis, the time domain is divided into a number of time intervals, separated by time steps. At time step t_{n-1} all nodal displacements, total strains, nonmechanical strains, and stresses in every part of the structure are known. The increments of nonmechanical strain due to creep and shrinkage of concrete and temperature changes occurring during time steps t_{n-1} and t_n are evaluated as explained in the section headed 'Material Constitutive Equations.

At each section, incremental forces due to nonmechanical strains are obtained by sectional integration. Such forces, added to the sectional prestressing primary forces existing if any prestressing operation is carried out at the beginning of the current time interval, are integrated over the member length so that the incremental initial stress load vector $\Delta\vec{F}^0$ is obtained. A similar procedure is followed for the sectional forces due to loads applied over the member length, obtaining the term $\Delta\vec{F}^*$.

Finally, the unbalanced-load vector $\Delta\vec{F}^u$ from the last time step is added, so that the load increment $\Delta\vec{F}_n$ at time step t_n to be applied to the structure is obtained by

$$\Delta\vec{F}_n = \Delta\vec{F}_n^{ext} + \Delta\vec{F}_n^u + \Delta\vec{F}^* + \Delta\vec{F}_n^0 \tag{8}$$

The total load increment may be divided into several smaller load increments for incremental load analysis. Unbalanced load iterations can be performed following standard iterative procedures, with or without changing the structural stiffness matrix.

Model 2: Panel Beam with Coupled Torsional-Flexural Behavior

Structural Idealization

The structure is divided longitudinally into a number of short, straight elements connected by nodes. Inside each element, a short number of integration sections is considered. Loads or moments must be applied only at the structural nodes.

With such a longitudinal scheme, a large number of joints is necessary to idealize medium-sized structures; nevertheless, the longitudinal integration along the elements is extremely simple, making the global process of structural analysis probably faster than with Model 1.

The cross section is considered to be composed of panels (Figure 3), which can resist only normal and shear stresses in their middle plane. The position and thickness of the panel, as well as of the concrete cover, which is allowed to spall, are known. Also, several reinforcing steel layers with any orientation and a layer of transverse prestressing can be defined at each panel.

Longitudinal prestressing tendons are individually defined, giving their steel area, position, and slopes at the integration sections with respect to the longitudinal axis. The active effect of prestressing is introduced in this model by means of an initial strain in the prestressing steel, which is calculated taking into account the friction losses.

Material Properties

Concrete is assumed to be subjected to a biaxial stress state. Before cracking, a biaxial isotropic elastic constitutive model is used, with a variable modulus of elasticity. Given the panel strains ε_x, ε_y, and γ, the principal strains ε_1 and ε_2 and their orientation β at the middle plane are obtained by means of bidimensional elasticity equations.

Once the principal strains on the middle plane are known, as well as the curvature in their direction induced by bending and torsion (7), the principal strains throughout the panel thickness can be obtained (Figure 3). Then the stress ratio α is

$$\alpha = \frac{\sigma_1}{\sigma_2} = \frac{\varepsilon_1 + \nu\varepsilon_2}{\varepsilon_2 + \nu\varepsilon_1} \tag{9}$$

where ν is Poisson's ratio, assumed constant.

With such a value, the ultimate stress and strain for the maximum compressive direction are determined, according to the Kupfer and Gerstle failure envelope (8) (Figure 4). By

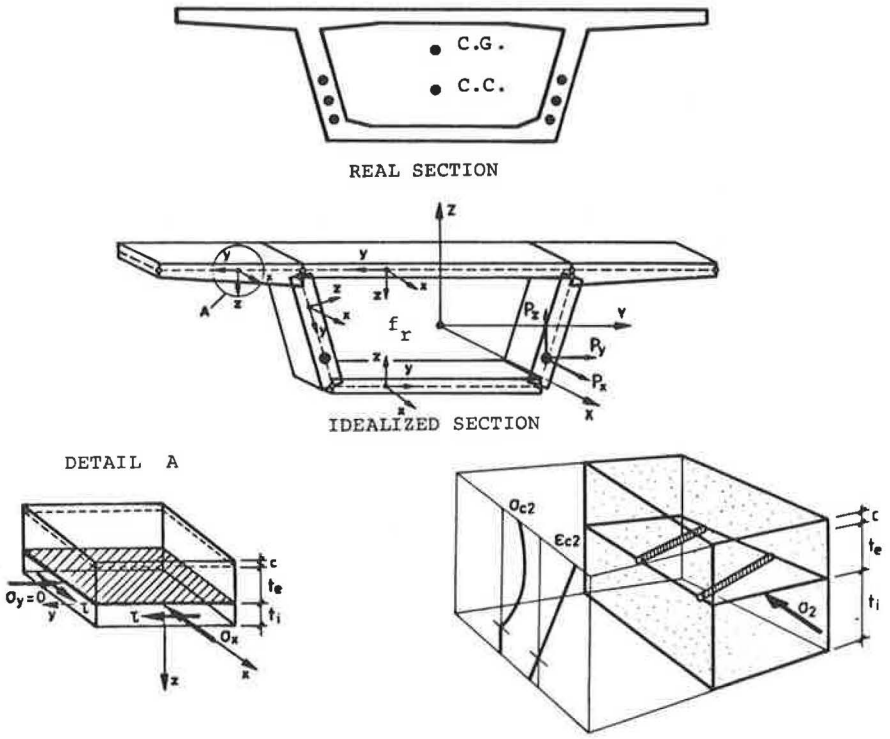

FIGURE 3 Structural idealization (Model 2).

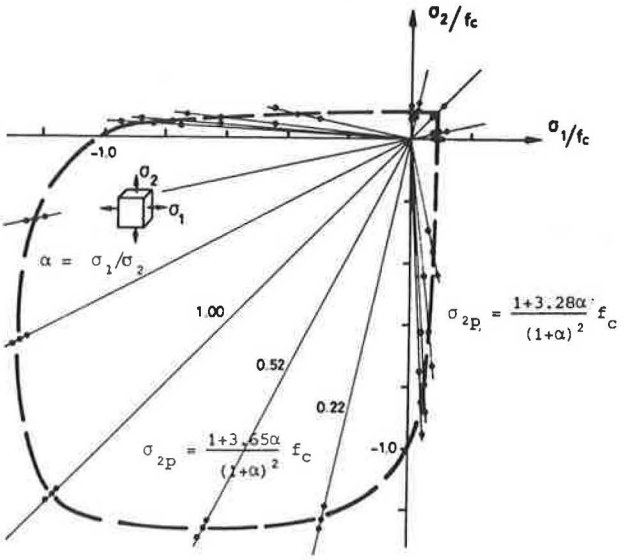

FIGURE 4 Failure envelope for concrete under biaxial stresses.

using Saenz's equation (*9*) to represent the concrete behavior, an apparent elasticity modulus for concrete is obtained:

$$E_a = \frac{\sigma_2}{\varepsilon_2} = \frac{E_{c0}}{1 + \left(\frac{E_{c0}\,\varepsilon_{2p}}{\sigma_{2p}} - 2\right)\left(\frac{\varepsilon_2}{\varepsilon_{2p}}\right) + \left(\frac{\varepsilon_2}{\varepsilon_{2p}}\right)^2} \tag{10}$$

The principal stresses are then

$$\sigma_1 = \frac{E_a}{1 - \nu^2}(\varepsilon_1 + \nu\varepsilon_2)$$

$$\sigma_2 = \frac{E_a}{1 - \nu^2}(\varepsilon_2 + \nu\varepsilon_1) \tag{11}$$

For cracked concrete, the evolutive truss analogy with stress reduction, according to Vecchio and Collins (*10*), is adopted to represent the panel behavior. In such a case, the ultimate stress and strain for the maximum compressive direction are determined by the following equations:

$$\sigma_{2p} = \frac{f_c}{\lambda} \qquad \varepsilon_{2p} = \frac{\varepsilon_{c0}}{\lambda}$$

$$\lambda = \left(\frac{\gamma m}{\varepsilon_2} - 0.3\right)^{1/2} \qquad \gamma m = \varepsilon_1 - \varepsilon_2 \tag{12}$$

The stress in the direction orthogonal to the cracks is assumed to be zero.

For the reinforcing steel the same constitutive relations as those in Model 1 are assumed for the direction in which the layer is oriented. Prestressing steel is assumed to be subjected to uniaxial stress with a stress-strain relationship similar to that in Model 1.

Sectional Analysis

The sectional behavior is governed by three sets of fundamental relationships: (a) compatibility between panel strains and sectional deformations, (b) constitutive relationships of the materials, and (c) equilibrium between sectional forces and stresses over the panels.

It is not possible to arrive, in this model, at an explicit constitutive equation at the sectional level, such as the one expressed for Model 1 by Equation 3. Then, to solve the sectional analysis, the process is the following:

1. The strains at each point of the section are obtained, by means of geometrical relationships, from the six general sectional deformations assuming Navier's plane-section hypothesis and nondeformability of sections in their plane;
2. Once the strains are known, stresses are obtained by means of the constitutive relationships of the materials (see previous section); and
3. Sectional forces are obtained by integration of stresses over the panels.

It is remarkable to note that this model does not separate torsional, flexural, axial, and shear behavior, making it possible to accurately predict the sectional response under combined actions. It is possible to capture failures due to crushing of concrete compression trusses, yielding of transverse steel, or yielding of longitudinal steel, depending on the load combinations.

Structural Analysis

The structural analysis method used in this model is essentially the same as that for Model 1, taking into account the particularities of the structural idealization (straight elements, loads applied only at structural joints, etc.). Unbalanced forces and prestressing effects are introduced as the initial stress loading vector. No time-dependent effects are considered in this model.

STRUCTURAL RESPONSE OF CURVED PRESTRESSED BOX GIRDER BRIDGE

The objectives of the present study are to show the capabilities of both analytical models, to compare their results when applied to the analysis of the same structure, and to study the response of a prestressed concrete box girder bridge under different loading conditions.

Description of Bridge Analyzed

The structure chosen for the present study is a curved prestressed concrete bridge actually constructed in Pamplona, Spain, in 1975 (*11*). The bridge superstructure consists of a three-span continuous beam whose total length is 88 m (28 m + 32 m + 28 m), with both ends torsionally fixed, supported without intermediate diaphragms over two single piers without torsional restraint. The geometry in plan consists of a circular curve of 120-m radius, followed by a spiral of parameter A = 80 (see Figure 5).

The cross section is a single box with side cantilevers 3.10 m long, making a total platform width of 12.85 m. The bottom slab is 5.75 m wide and the webs, 0.70 m thick, are included with a 2/1 slope. The bridge has a constant depth of 1.30 m, a top-deck constant thickness of 0.24 m, and a bottom-deck thickness of 0.20 m that increases to 0.35 m over the supports (see Figure 6).

The longitudinal prestressing is composed of 26 tendons 12T13 of 346 cm^2 total area, anchored in both ends of the superstructure by means of stressing anchorages. Because of the platform width and the large torsional span, which causes high stresses near the abutments, the top and bottom slabs are transversely prestressed along the final 7 m by means of tendons of 12 ϕ7 separated 0.67 m and 0.51 m, respectively.

The structure was constructed by means of a framework, directly soil supported, extended along the whole bridge length.

Idealization of Bridge and Analyses Performed

The centerline of the bridge was idealized as a circular curve of 120-m radius. The transverse and longitudinal discretizations are shown in Figure 7. Two equivalent tendons are

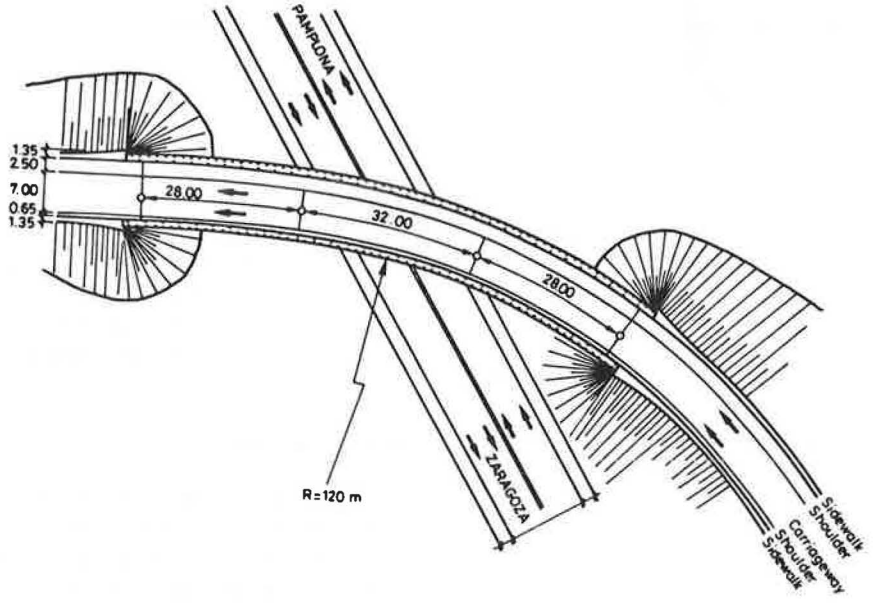

FIGURE 5 General plan of the bridge.

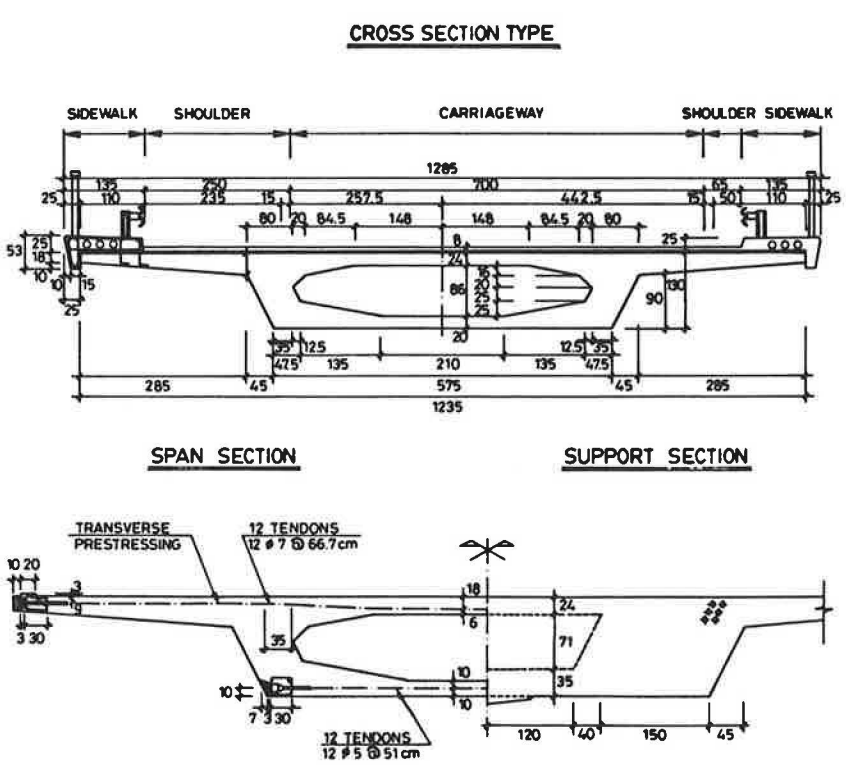

FIGURE 6 Cross section of the bridge.

used to represent the longitudinal prestressing with a total anchorage force of 19 000 kN each. The tendon layout is shown in Figure 8. For analysis purposes, the reinforcing steel arrangement has been divided into four zones, described in Figure 8.

Concrete properties assumed for the analysis are initial modulus E_c = 36 000 MPa; compressive strength f_c' = 35 MPa; tensile strength f_t = 3.5 MPa; peak strain $\varepsilon_0 = -0.002$; and ultimate strain $\varepsilon_u = 0.0035$. The reinforcing steel properties assumed are initial modulus E_s = 210 000 MPa; no strain hardening; strength f_s = 410 MPa; and ultimate strain ε_{su} = 0.01. The prestressing steel has been assumed to have an initial modulus E_p = 200 000 MPa; a yielding stress f_{py} = 1500 MPa; and a strength $f_{p\max}$ = 1700 MPa.

Time-dependent properties of concrete have been considered according to the Model Code of the Comité Euro-International du Béton and International Federation of Prestressed Concrete (CEB-FIP) (*12*), assuming a medium ambient humidity (50 percent), no shrinkage strain, and a constant temperature of 20°C. The concrete strength is assumed to increase with time, from 35 MPa at t = 30 days to 50 MPa at t = 10,000 days. Also the deformational modulus varies, from E_c = 36 000 MPa to E_c = 42 400 MPa, so that aging of concrete is taken into account. The final relaxation of the prestressing steel is assumed to be 5 percent of the initial stress. Transverse prestressing tendons are assumed to be initially stressed at 70 percent of their yielding stress.

No anchorage slip has been considered. Friction coefficients adopted are $\mu = 0.20$ and $k = 0.0012$. Jacking is assumed to be done from both ends simultaneously.

The loads considered in the analysis are the self weight of the bridge (*SW*), a dead load (*DL*) of 2.0 kN/m^2, and a live load (*LL*) of 4.0 kN/m^2 that can be extended to any surface and length of the bridge. No truck loads have been considered in the analysis. The following loading cases have been considered:

Load Case 1: *SW* + *DL* + *LL* extended over the whole bridge length and width.

Load Case 2: *SW* + *DL* + *LL* extended over the whole bridge length and the exterior half-width only.

Load Case 3: *SW* + *DL* + *LL* extended over the whole bridge length and the interior half-width only.

The analyses performed are the following:

Analysis 1: short-term (t = 30 days after casting); Models 1 and 2; Load Case 1 with increment of *LL* to failure.

Analysis 2: short-term (t = 30 days after casting); Models 1 and 2; Load Case 2 with increment of *LL* to failure.

Analysis 3: short-term (t = 30 days after casting); Models 1 and 2; Load Case 3 with increment of *LL* to failure.

Analysis 4: time-dependent; only Model 1; Load Case 1; *SW* at 30 days, *DL* at 60 days, *LL* at 10,000 days increasing to failure.

Analysis 5: short-term (t = 30 days after casting); Models 1 and 2; Load Cases 1, 2, and 3, including transverse prestressing.

Results of Analyses

Analysis 1: Centered Live Load

Figure 9 shows the load-deflection and load-force curves, respectively, for that case. Cracking appears in the support

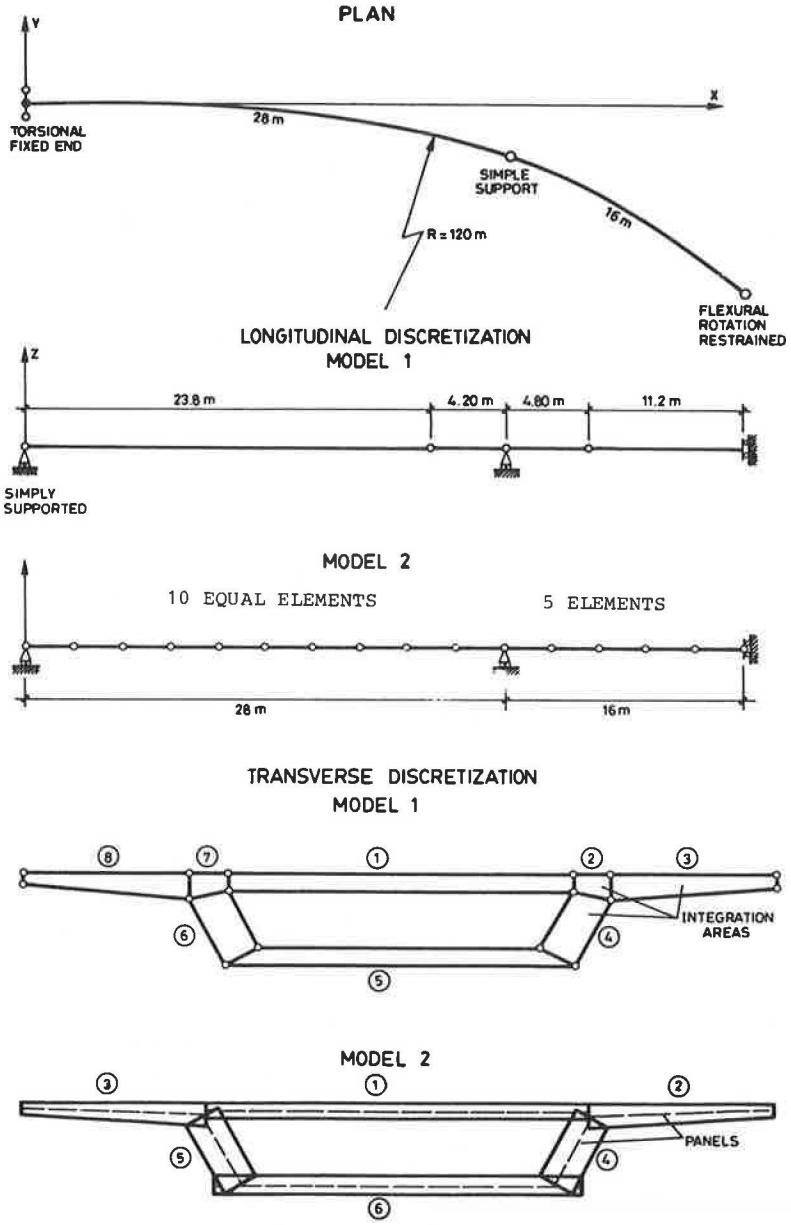

FIGURE 7 Longitudinal and transverse idealization of the bridge.

section at about 8.0 times the live load, whereas flexural rupture due to prestressing steel yielding in the same section is produced at approximately 11.5 times the *LL*.

A very small redistribution of forces takes place for this loading case. The bending moment at the middle of the central span decreases, whereas in the support section a 4 percent increase takes place in the ultimate state.

In general, good agreement is obtained between the results of both models, which indicates that for dominant flexural behavior, the uncoupled model can be used with reasonable accuracy in these kinds of structures.

Analysis 2: Eccentric External Live Load

In this case, the opposite situation is found: the torsional behavior is dominant, and bending moments are very small. Figure 10 shows the load-deflection and load-force curves. Cracking appears at the abutments because of the important torsional moment acting, at 4 times the live load, according to Model 1. Model 2 predicts cracking at a higher value of the overload factor. Such a difference is due to the effect of shear stresses coming from external loads and to the prestressing slope at the end of the beam, both of which are taken into account in Model 2. After cracking, a reduction of the moment at the middle of the central span and an increase of the support moment are produced with increasing load. Such a redistribution of bending moments that are due to the variation of the *EI/GJ* ratio along the bridge reaches 66 and 37 percent at the center and support sections, respectively, when failure occurs. Model 2 also predicts a sudden increase of the central deflection after cracking. Failure occurs at about 8.8 times the live

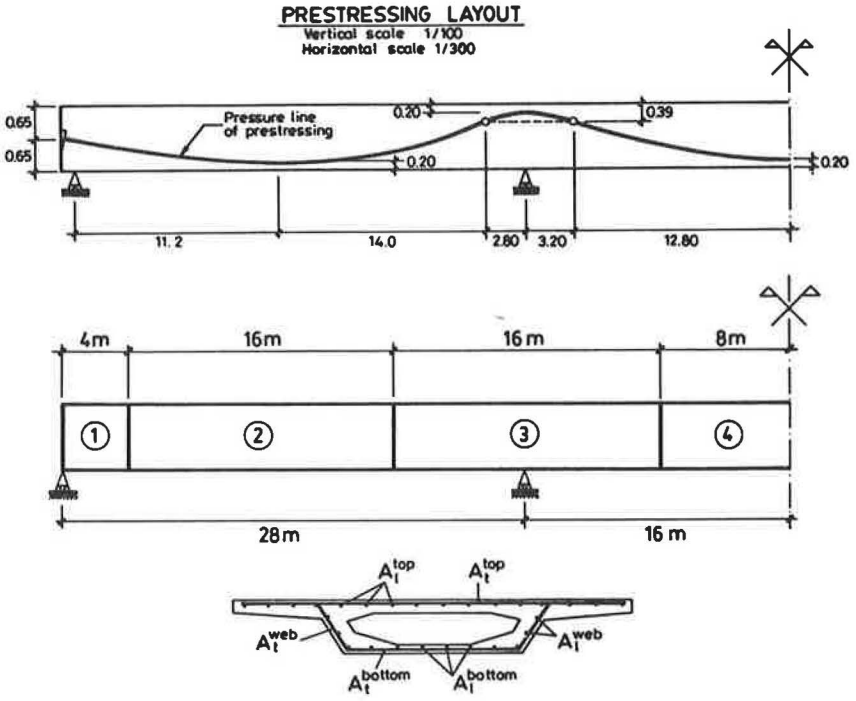

	LONGITUDINAL REINFORCEMENT cm^2/m			TRANSVERSE REINFORCEMENT cm^2/m		
ZONE	A_l^{top}	A_l^{bottom}	A_l^{web}	A_t^{top}	A_t^{bottom}	A_t^{web}
1	28.0	40.0	28.0	28.0	28.0	85.2
2	21.0	40.0	21.0	21.0	21.0	77.0
3	27.2	12.3	12.3	12.3	12.3	132.0
4	3.8	24.0	3.8	3.8	60.0	3.8

FIGURE 8 Prestressing and reinforcing steel arrangement adopted for the analysis.

load, when the ultimate torque is reached at the abutments, because of yielding of the transverse reinforcement.

In general there is excellent agreement between the results of both models, which indicates that even when torsional behavior is dominant, the uncoupled model provides good results.

Analysis 3: Eccentric Interior Live Load

Figure 11 shows the load-deflection and load force curves for this analysis. Good agreement is obtained also, although differences are a little larger than those under other loading conditions.

Failure at the abutments due to torsion is reached at practically the same time as flexural rupture in the central span section, at approximately 11.8 times the live load. Cracking is detected in both models at about 7.0 times the live load. Then a redistribution of bending moments opposite the one produced in Analysis 2 occurs for the same reason. The bending moment in the support section is about 30 percent smaller than the elastic value in the ultimate state.

In this bridge the sections subjected to maximum torque and maximum bending moment are different and very separated. Practically no cross section is being subjected simultaneously to torsion and bending of similar importance. Therefore, the uncoupled model can be used for any load combination with reasonable accuracy, because there is no deformational interaction between torsion and bending at any section.

Analysis 4: Time-Dependent Analysis

The objective of such an analysis is, on one hand, to determine the influence of time-dependent effects on the ultimate load capacity of the bridge, assuming no evolutive construction. On the other hand, a comparison of the computer results and the ones made by hand for design purposes is established.

Figure 12 shows the time-deflection diagram for the middle of the central span. From that curve it can be seen that the central deflection, after the dead load has been applied, remains practically constant with time, with a slight tendency to decrease, which means that prestressing and permanent loads are equilibrated.

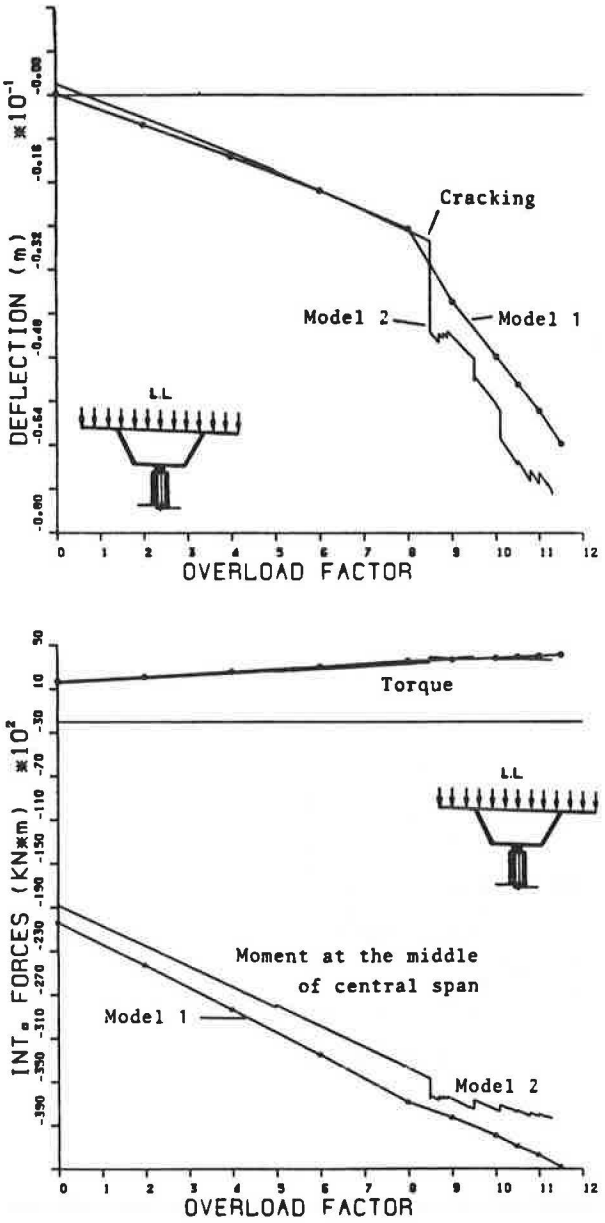

FIGURE 9 Results of Analysis 1.

The small redistribution of bending moments that occurs with time is due to the existence of prestressing and reinforcing steel on the compression side, which restrains the time deformation of concrete by increasing its compressive stress about three times (Figure 13).

The force along the three tendons is shown in Figure 14 for different times. It can be observed that, in addition to a general decrease of the tendon force because of creep and relaxation losses, there is a tendency to lose uniformity of the force along the tendons. A total loss of 3700 kN at the middle of the central span (about 12.5 percent) is obtained, which is a little lower than the results obtained by hand calculation (no shrinkage is taken into account in this analysis).

Figure 15 shows load-deflection curves at 30 and 10,000 days for a centered live load increasing to failure. From these curves it can be seen that ultimate capacity is constant with time and that cracking is advanced because of the loss of prestressing force.

Analysis 5: Transverse Prestressing

The objective of this analysis is to use Model 2 to study the influence of transverse prestressing of the top and bottom slabs near abutments on the structural response of the bridge under the three loading cases. Transverse prestressing is designed to avoid a great decrease in the torsional rigidity under high torsional moments, which may produce important variations in the longitudinal bending moments.

Figure 16 shows redistribution of the bending moments at the support section for the three loading cases, with and

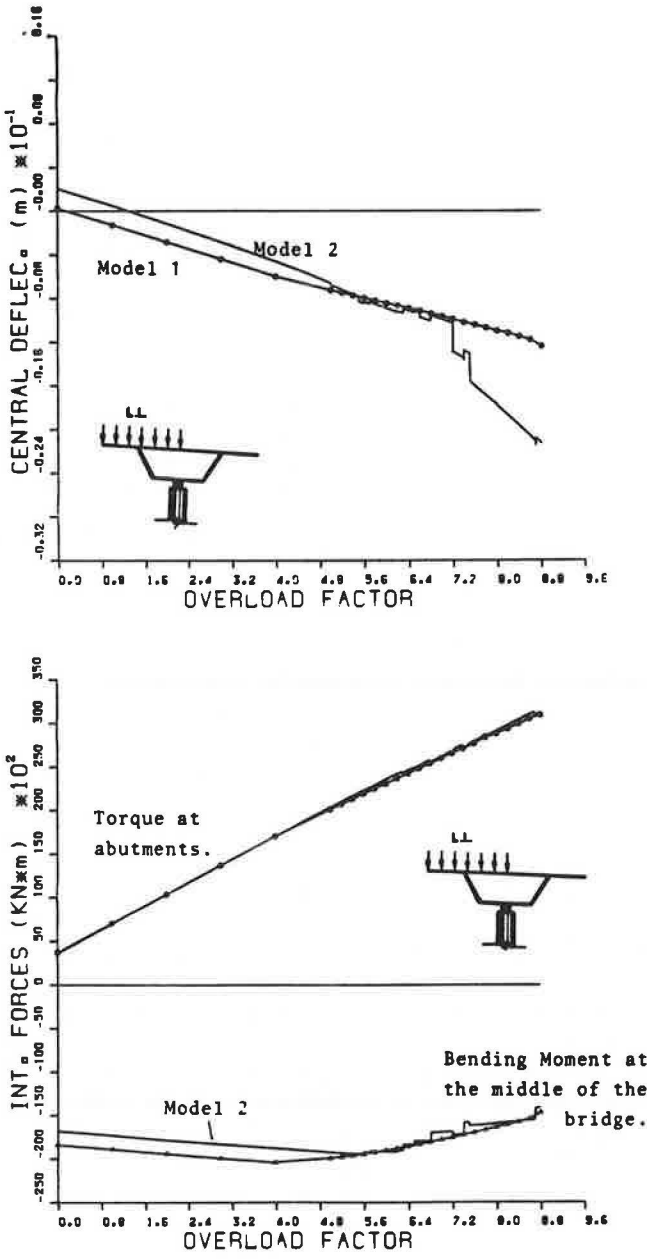

FIGURE 10 Results of Analysis 2.

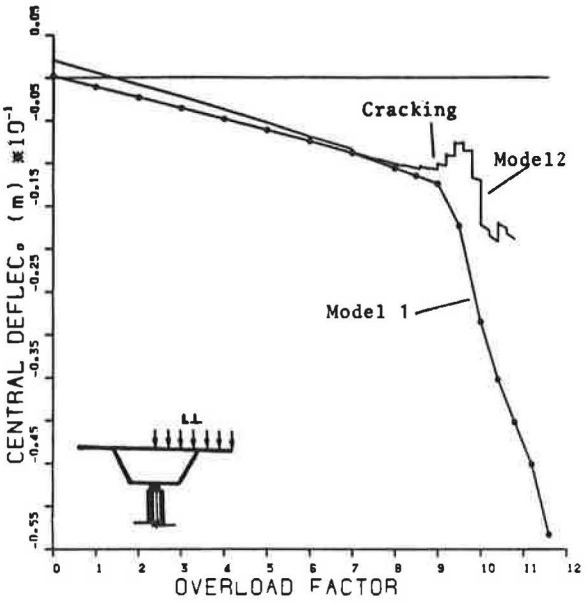

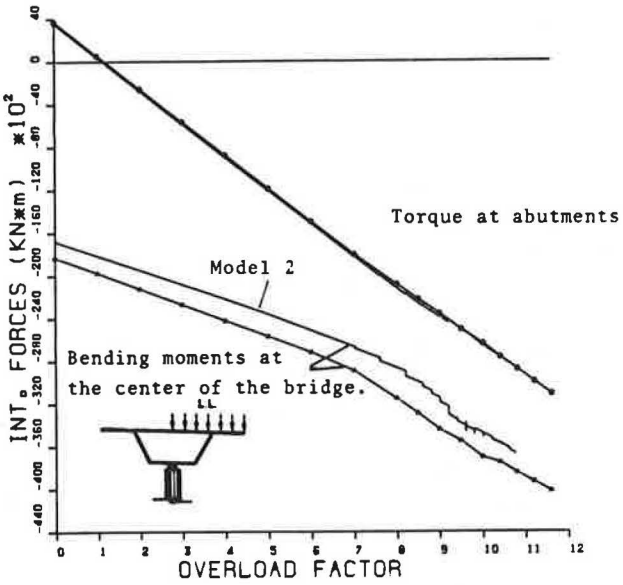

FIGURE 11 Results of Analysis 3.

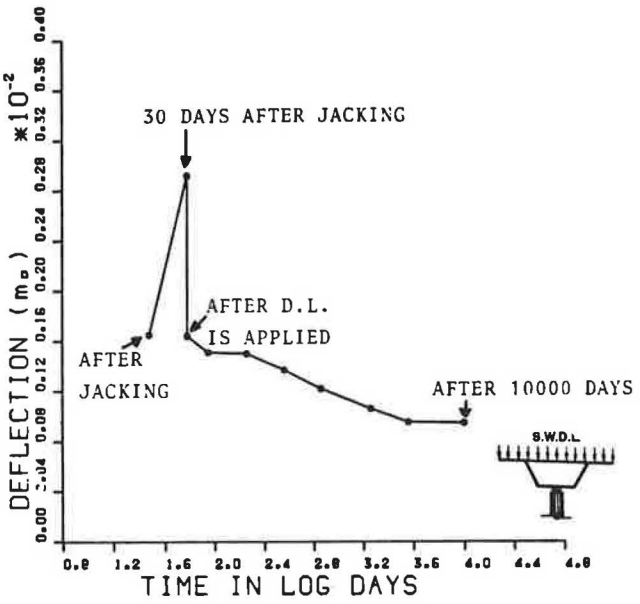

FIGURE 12 Deflection at the middle of the central span.

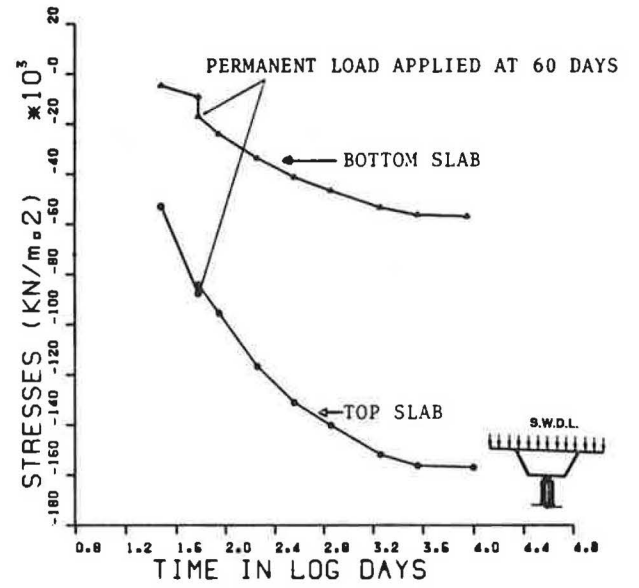

FIGURE 13 Stresses in the longitudinal reinforcing steel over the support versus time.

without transverse prestressing. It can be seen that the cracking load is slightly increased by transverse prestressing and the ultimate load capacity remains the same.

CONCLUSIONS

1. The structural response of curved prestressed box girder bridges supported over intermediate piers without torsional restraints is highly nonlinear after cracking under increasing loads.

2. The kind and degree of redistribution of internal forces depend, essentially, on the loading cases considered. For an external live load, a 37 percent increase in the bending moment over the support occurs at failure. For a centered live load such an increase is only 4 percent, whereas for an internal eccentric live load a decrease of about 30 percent takes place for the bridge studied.

3. The kind of failure depends on the load case considered. For a centered overload, flexural rupture takes place; for an external live load the failure is due essentially to torsion at the bridge ends; and for an internal overload, failure occurs simultaneously by flexural rupture at the support section and by torsion at the abutments.

4. When there is no evolutive construction, the ultimate load capacity of the bridge remains constant with the passage of time. However, the cracking load may be reduced because of prestressing losses. Redistribution of moments takes place with time because of the restraint that the reinforcing and prestressing steel introduces in the deformation of the section.

5. Transverse prestressing of top and bottom slabs introduces variations in the cracking load. However, it has no

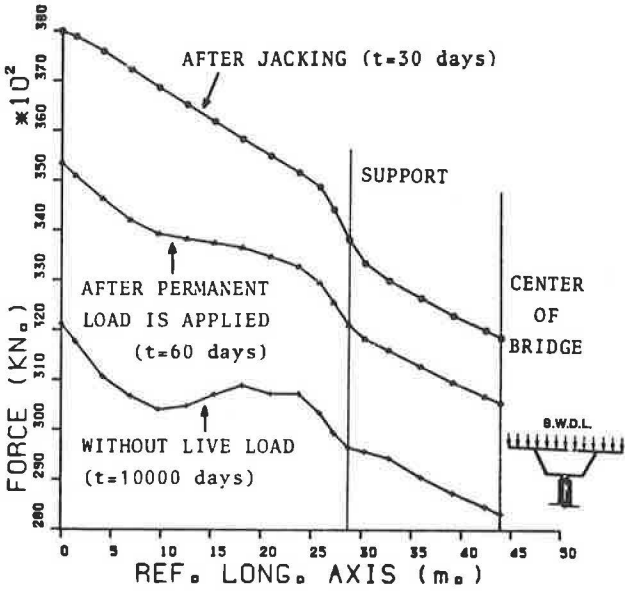

FIGURE 14 Tendon force along the bridge length at different times.

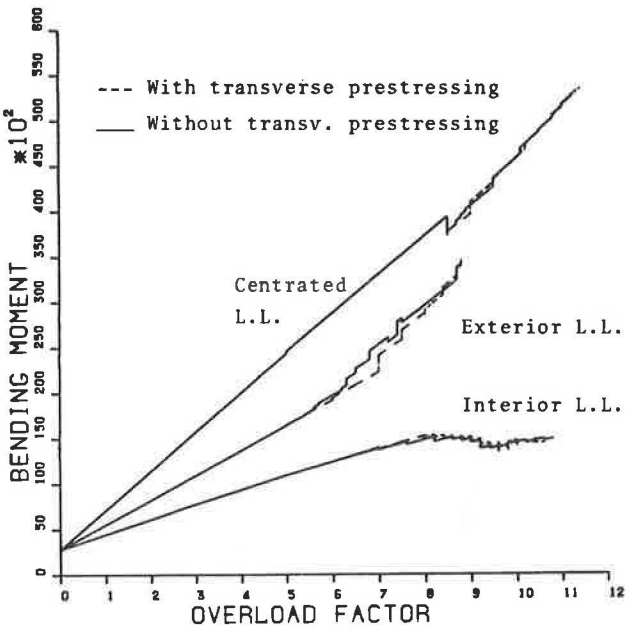

FIGURE 16 Bending moments at the support section (Analysis 5).

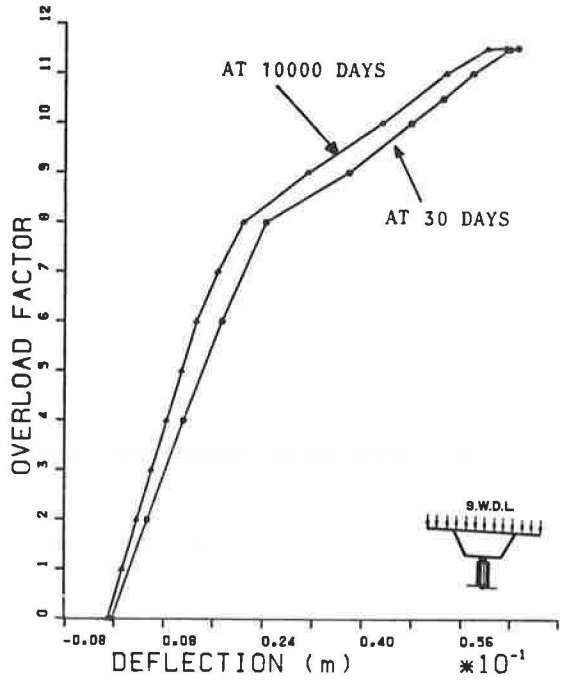

FIGURE 15 Live load deflection at the middle of the central span.

noticeable influence over the ultimate load capacity if the total mechanical ratio of transverse steel remains constant.

6. When either torsion or bending is dominant, uncoupled models can be used to predict the nonlinear response of reinforced and prestressed concrete structures. This circumstance occurs for the curved bridge studied, where, in addition, the sections subjected to maximum bending moment and maximum torque are different.

7. However, in other kind of structures, such as straight skew bridges or longer curved bridges with or without intermediate torsional restrained supports, bending and torsion interact on the same sections. Then coupled models must be used to simulate the structural behavior.

ACKNOWLEDGMENTS

The research reported in this paper was carried out at the Universitat Politècnica de Catalunya, Barcelona, Spain. Part of this work was done in cooperation with the University of California, Berkeley, in Project CCA-8309/012, sponsored by the U.S.-Spain Joint Committee for Scientific and Technological Cooperation. The Computer Center at the Department of Civil Engineering of the Universitat Politècnia de Catalunya provided the facilities for the numerical work. The authors wish to express their gratitude to A. C. Aparicio, codesigner of the bridge studied in this paper, for his help in providing the data necessary to carry out the analyses.

REFERENCES

1. S. Carrascón, A. R. Marí, and I. Carol. *Nonlinear Time Dependent Analysis of Curved Reinforced and Prestressed Bridges* (in Spanish). Report ES-015. Department of Civil Engineering, Universitat Politècnica de Catalunya, Barcelona, Spain, March 1987.
2. A. Lopez. A Study of the Behavior Under Increasing Loads, up to Failure, of Curved or Skew Continuous Prestressed Concrete Bridge Decks (in Spanish). Ph.D. thesis. Department of Civil Engineering, Universitat Politècnica de Catalunya, Barcelona, Spain, March 1987.
3. J. Manterola. *Opened and Closed Sections Under Eccentric Loading* (in Spanish). Monografía 15. Agrupación de Fabricantes de Cemento de España, 1976.
4. M. Sargin. *Stress-Strain Relationship for Concrete and the Analysis of Structural Concrete Sections.* Study No. 4. Solid

Mechanics Division, University of Waterloo, Waterloo, Ontario, Canada, 1970.
5. Y. J. Kang and A. C. Scordelis. Nonlinear Analysis of Prestressed Concrete Frames. *Journal of the Structural Division,* ASCE, Vol. 106, No. ST2, Feb. 1980.
6. P. Lampert. Postcracking Stiffness of Reinforced Concrete Beams in Torsion and Bending. In *Special Publication 35.* American Concrete Institute, Detroit, Mich., 1973.
7. M. Pre. Etude de la torsion dans le béton precontraint par la méthode du treillis spatial evolutif. *Annales de l'Institut Technique du Bâtiment et des Travaux Publics,* No. 385, July-Aug. 1980.
8. H. B. Kupfer and K. H. Gerstle. Behavior of Concrete under Biaxial Stresses. *Journal of the Engineering Mechanics Division,* ASCE, Vol. 99, No. EM4, Aug. 1973.
9. L. P. Saenz. Discussion of Equation for the Stress-Strain Curve of Concrete by Desay and Krishnan. *Journal of the American Concrete Institute,* Vol. 61, Sept. 1964.
10. F. Vecchio and M. P. Collins. Stress-Strain Characteristics of Reinforced Concrete in Pure Shear. Presented at International Association for Bridge and Structural Engineering Colloquium on Advanced Mechanics of Reinforced Concrete, Delft, Netherlands, 1981.
11. J. J. Arenas and A. C. Aparicio. Paso superior en la carretera de Zaragoza. Autovía Ronda Oeste de Pamplona. *Realizaciones Españolas,* ATEP, pp. 30–33, 1975.
12. Comité Euro-International du Béton and International Federation of Prestressed Concrete. *CEB-FIP Model Code for Concrete Structures.* American Concrete Institute, Detroit, Mich., 1978.

Publication of this paper sponsored by Committee on Concrete Bridges.